Microchimica Acta (2021) 188:285
https://doi.org/10.1007/s00604-021-04939-2

ORIGINAL PAPER

Ultrasensitive electrochemical detection of hepatitis C virus core antigen using terminal deoxynucleotidyl transferase amplification coupled with DNA nanowires

Yuwei Wang[1,2] · Linbin Li[1,2] · Zihe Dong[1,2] · Yan Yu[1,2] · Aie Zhou[1,2] · Xiaofen Zhao[1,2] · Juan Zhang[1,2]

Received: 16 February 2021 / Accepted: 9 July 2021

Abstract

Early diagnosis of hepatitis C virus (HCV) infection is essential to prevent disease from spreading and progression. Herein, a novel electrochemical biosensor was developed for ultrasensitive detection of HCV core antigen (HCVcAg) based on terminal deoxynucleotidyl transferase (TdT) amplification and DNA nanowires (DNW). After sandwich-type antibody-antigen recognition, the antibody-conjugated DNA was pulled to the electrode surface and further extended into a long DNA sequence by robust TdT reaction. Then, large numbers of methylene blue–loaded DNW (MB@DNW) as signal labels are linked to the extended DNA sequence. This results in an amplified electrochemical signal for HCVcAg determination, typically measured at around −0.25 V (Ag/AgCl). Under the optimum conditions, the proposed biosensor achieved a wide linear range for HCVcAg from 0.1 to 312.5 pg/mL with a low limit of detection of 32 fg/mL. The good practicality of the biosensor was demonstrated by recovery experiment (recoveries from 98 to 104% with RSD of 2.5–4.4%) and comparison with enzyme-linked immunosorbent assay (ELISA). Given the highlighted performance, the biosensor is expected to act as a reliable sensing tool for HCVcAg determination in clinics.

Keywords Hepatitis C virus · HCV core antigen · Electrochemical biosensor · Terminal deoxynucleotidyl transferase amplification · DNA nanowires

Introduction

Hepatitis C virus (HCV) has infected more than 170 million people throughout the world [1–3]. The HCV core antigen (HCVcAg) can be detected in serum or plasma within 1 week after HCV infection [4], while HCV antibodies have a long window period of 2–6 months [5, 6]. Therefore, HCVcAg is regarded as an effective biomarker for early diagnosis of HCV infection [7, 8].

Currently, enzyme-linked immunosorbent assay (ELISA) based on HRP enzyme has been reported for HCVcAg analysis [6, 9]. However, ELISA method suffers from low sensitivity. Recently, some novel strategies have been constructed for HCVcAg detection. For example, Roushani's group developed several HCVcAg electrochemical biosensors using different nanomaterials, including TiO_2-doped celestine blue tag [10], vanadium oxide nanobelts [11], silver nanoparticle and thiol graphene quantum dots nanocomposite [12], and multi-walled carbon nanotubes-chitosan nanocomposite [13]. In another study, Zhou's group engineered a plasmonic HCVcAg nanoplatform composed of catalytic hairpin assembly–induced G-quadruplex/hemin DNAzyme and nanofibrous membrane [14]. Although these strategies possessed high sensitivity, certain defects still remain: (i) the synthesis of the nanocomposite needs multiple steps, resulting in time-consuming preparation process; and (ii) it is hard to control the same size of the nanocomposite in different batches, leading to the poor repeatability of the biosensors [15]. Thereby, there is a need for methods that enable simple, accurate, and ultrasensitive analysis of HCVcAg.

✉ Xiaofen Zhao
zhaoxiaofen0813@163.com

✉ Juan Zhang
juanmcq@163.com

[1] Department of Laboratory Medicine, Chongqing Hospital of Traditional Chinese Medicine, Chongqing 400016, China

[2] Chongqing Key Laboratory of Sichuan-Chongqing Co-construction for Diagnosis and Treatment of Infectious Diseases Integrated Traditional Chinese and Western Medicine, Chongqing Hospital of Traditional Chinese Medicine, Chongqing 400016, China

Published online: 03 August 2021

Using deoxyribonucleic acid (DNA) as architecture component to construct signal amplification strategies has gained increasing attention in developing high-performance biosensors owing to its precise base pairing [16, 17]. Accordingly, various strategies have been used to analyze cells, nucleic acids, and proteins [18, 19]. These strategies are mainly spitted into two groups: dynamic systems that can change the structure of substrates in response to target (catalytic hairpin assembly, rolling circle amplification, terminal deoxynucleotidyl transferase (TdT) amplification, and so forth) and static framework devices that structure of their substrates remains unchanged (origami and nanotube) [20, 21]. Among them, TdT amplification and DNA nano-frameworks are noteworthy events. Specifically, TdT is a protein enzyme responsible for introducing extra nucleotides into DNA strands without the need for a template sequence, which is recognized as a potential tool for controlled DNA synthesis [22–24]. The bases of the synthesized DNA strands can be easily adjusted by changing the constitution of the substrate deoxyribonucleoside triphosphate (dNTP) [25–27]. For DNA nano-frameworks, several signal labels have been developed based on tetrahedron [28], nanosheet [29], and dendrimer [30]. Different from three-dimensional structures, one-dimensional DNA nanotubes or nanowires possess unique structural and functional properties, such as tunable geometry [31], high aspect ratio [32], high cargo encapsulation [33], and precise cargo anchorage [34]. This makes one-dimensional DNA materials have a high level of signal label loading capability. Therefore, TdT amplification strategy and DNW are attractive tools for the construction of biosensors for sensing HCVcAg.

Herein, we developed a novel electrochemical biosensor for ultrasensitive HCVcAg analysis, combining TdT amplification and DNW. This periodically ordered DNW was one-step assembled from only four short single-stranded DNA, which enabled a label-free and efficient load of methylene blue (MB) to form MB@DNW signal tag (Scheme 1A). Target HCVcAg recognized Ab_1 immobilized on the electrode surface and DNA-tagged Ab_2 (DNA-Ab_2). The DNA was then added poly(T) sequence at its 3′ end extended by TdT using thymidine as substrate. The extended DNA hybridized with MB@DNW, producing an amplified signal for detection of HCVcAg (Scheme 1B). The proposed strategy did not need additional nanomaterials, possessing appealing advantages of simple operation and good repeatability.

Experimental section

Materials and reagents

Bovine serum albumin (BSA), 25-bp DNA marker, and DNA oligonucleotides (listed in Table S1) were obtained from Sangon Inc. (Shanghai, China). Monoclonal HCVcAg antibodies (Ab_1) and polyclonal HCVcAg antibodies (Ab_2) were purchased from ViroStat, Inc. (Portland, USA). Sulfosuccinimidyl-4-(*N*-maleimidomethyl) cyclohexane-1-carboxylate (SMCC), dithiothreitol (DTT), and MB were gained from Sigma-Aldrich (USA). 2′-Deoxythymidine 5′-triphosphate (dTTPs) was obtained from ThermoFisher Scientific. Terminal deoxynucleotidyl transferase (TdT) and 10× TdT buffer were purchased from Beyotime Biotechnology (Shanghai, China). PBS_1 buffer (pH 7.40) contained 55 mM Na_2HPO_4, 55 mM NaH_2PO_4, 150 mM NaCl, and 20 mM EDTA. PBS_2 buffer (pH 7.40) contained 55 mM Na_2HPO_4, 55 mM NaH_2PO_4, 150 mM NaCl, and 5 mM EDTA. The thiolated DNA was dissolved in 10 mM Tris-HCl buffer (pH 8.0) containing 1 mM EDTA. All other reagents were of analytical grade, and aqueous solutions were prepared using Milli-Q water (18 MΩ cm^{-1}).

Apparatus

CHI660D electrochemical workstation (Shanghai Chenhua Instruments Co., Ltd., China) was used to perform electrochemical experiments. The workstation has a three-electrode system including a working electrode (gold electrode with 3 mm diameter, GE), a counter electrode (platinum wire), and a reference electrode (Ag/AgCl). An ultraviolet–visible (UV–vis) spectrophotometer (Shimadzu, Kyoto, Japan) was used to characterize the features of DNA-Ab_2 conjugate and MB@DNW.

Synthesis of the DNA-Ab_2 conjugate

The DNA-Ab_2 conjugate was synthesized based on a coupling reaction between the sulfhydryl group of the thiolated DNA and amino group of the antibody according to the references [35, 36]. First, the Ab_2 solution was diluted to 0.2 mg/mL using PBS_1. To activate Ab_2, 50 μL of 0.4 mM SMCC in anhydrous DMSO was mixed with 500 μL of the prepared Ab_2 solution and incubated at room temperature for 2 h under shaking slightly. Subsequently, the activated Ab_2 was purified by ultrafiltration using a 100-kD Millipore (10,000 rpm, 10 min), and then dissolved in 500 μL of PBS_2. Second, 200 μL of 100 mM DTT was added into 150 μL of 100-μM thiolated DNA, and diluted with 2.5 mL of 55 mM PBS_1 for 1 h at 37 °C to reduce dimerization of the thiolated DNA. The reduced DNA was purified by ultrafiltration using a 10-kD Millipore (10,000 rpm, 10 min), and then dissolved in 500 μL PBS_2. Third, 500 μL of the reduced DNA was mixed with 500 μL of the activated Ab_2 solution, incubated overnight at 4 °C. Then, the unreacted DNA was removed by ultrafiltration using a 100-kD Millipore

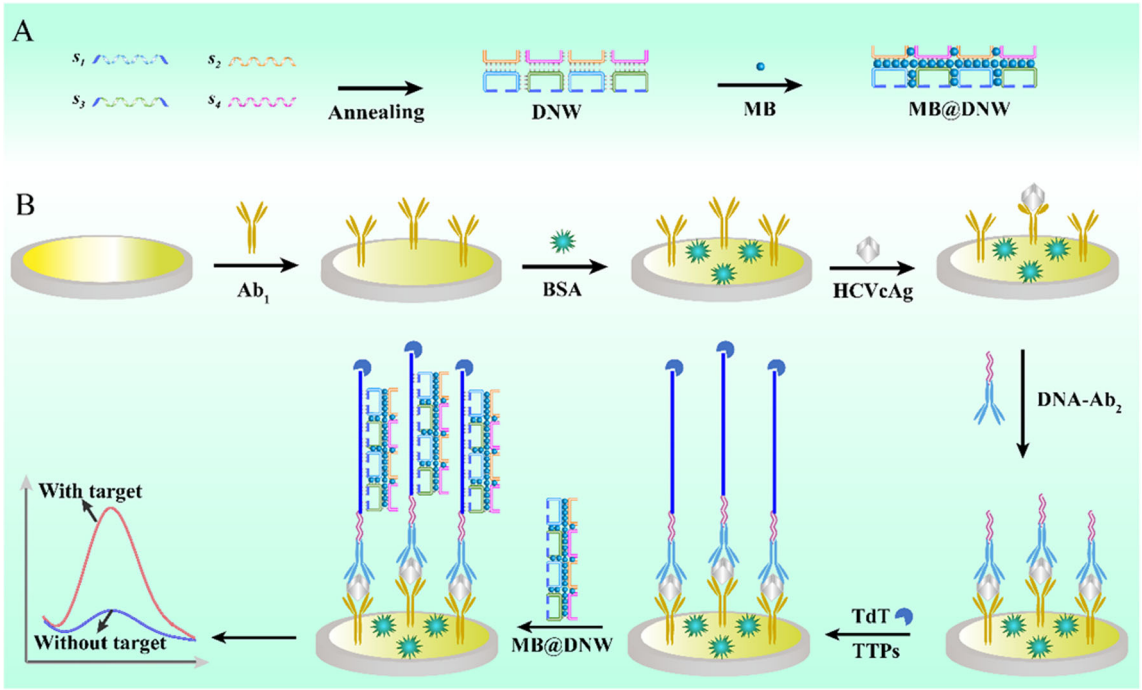

Scheme 1 Operation principle of the electrochemical biosensor for HCVcAg analysis. (**A**) the assembly procedure of MB@DNW and (**B**) the steps of DCP detection

(10,000 rpm, 10 min), and washed with PBS_1 at least 3 times. The remained DNA-Ab_2 conjugate was dissolved in 1.0 mL of PBS_2.

Preparation of the MB@DNW

The DNW consisted of four DNA strands (S1–S4). These strands were first mixed with correct stoichiometry at 4.0 μM in 1× TAE/Mg^{2+} buffer (40 mM Tris-Acetate, 1 mM EDTA, 12.5 mM $MgCl_2$, pH 8.0). The mixture was placed at 95 °C for 5 min, and then slowly cooled down to room temperature to form DNW nanostructure. Afterwards, 100 μL of MB (1.0 μM) was added into 20 μL of the mixture and incubated at 37 °C for 2 h under shaking to form the MB@DNW signal label. The prepared MB@DNW was stored at 4 °C before use.

Preparation of the GE

The bare GE was first polished with 0.3-μm alumina slurry. The polished GE was treated by ultrasonication in deionized water. Then, the electrode was immersed in a freshly prepared piranha solution (30% H_2O_2, 70% H_2SO_4) for 10 min, and rinsed thoroughly with deionized water to eliminate residues. Subsequently, 10 μL of Ab_1 (50 μg/mL) was dropped on the treated electrode surface and incubated at 4 °C overnight. After rinsing with PBS_1 buffer, the GE was incubated in 1% (w/v) BSA for 2 h to block nonspecific sites. The prepared GE was stored at 4 °C before use.

Immunoassay and electrochemical measurement

Various concentrations of HCVcAg were dropped onto the prepared GE and reacted for 30 min. Then, 10 μL of DNA-Ab_2 (20 nM) was dropped onto the electrodes and reacted for 30 min. Subsequently, the electrodes were loaded with 10 μL of the mixture containing 0.5 mM dTTPs, 5 U μL^{-1} TdT, and 1× TdT buffer, followed by reaction for 60 min. Furthermore, 10 μL of DNW was dropped onto these electrodes and incubated for 30 min. At each step, the electrodes were washed three times with Tris-HCl to remove unbound substances. Finally, the electrochemical measurements were performed with differential pulse voltammetry (DPV) in PBS. The DPV measurement conditions included scanning potentials ranging from −0.5 to 0 V, a potential step of 5 mV, a pulse amplitude of 50 mV, a pulse width of 50 ms, and a pulse period of 200 ms. For electrochemical impedance spectroscopy (EIS), the parameters included bias potential of 0.26 V and amplitude of 5 mV.

Polyacrylamide gel electrophoresis

A polyacrylamide gel electrophoresis (PAGE) experiment was performed on a DYY-6C electrophoresis analyzer (Liuyi Instrument Company, China) in 1× TBE buffer (pH 8.3, 89 mM Tris-boric acid, 2 mM EDTA) at 110 V for 50 min. After GoldView staining for 30 min, the prepared gel was imaged on a Bio-Rad ChemDoc XRS (Bio-Rad, USA).

Result and discussion

Characterization of DNA nanowires and DNA-Ab_2

First, the designed DNW was characterized by using PAGE. As shown in Fig. 1A, compared to the S1 strand in lane 1, the hybridization of S1 and S2 (lane 2) and the hybridization of S3 and S4 (lane 3) appeared a new band with slower mobility. When they were mixed together at the same concentration, the main DNA strands were located in the top band (lane 4), suggesting the successful assembly of DNW. Furthermore, the loading efficiency of the designed DNW toward MB was evaluated. As shown in Fig. 1B, the UV–vis adsorption value of MB (1.0 μM) at 680 nm gradually decreased with increasing the concentration of DNW from 160 to 240 nM, and then had an ignorable change even at the higher DNW concentration. These results indicated that 1.0 μM of MB could have been almost entirely loaded into 240 nM of DNW, demonstrating the good loading efficiency of the DNW toward MB. In addition, the prepared DNA-Ab_2 was characterized. As shown in Fig. S1, compared with a typical peak of DNA at 260 nm (curve a) and a representative peak of the Ab_2 at 280 nm (curve b), a merged peak at 260 nm was observed in the absorption spectrum of the synthesized DNA-Ab_2. The result indicated that the DNA was successfully bound to Ab_2. Based on the absorbance ratio (260 nm vs 280 nm) [37, 38], five DNA strands were tethered to an antibody in DNA-Ab_2.

Valuation of the feasibility of the electrochemical biosensor

To verify the feasibility of the electrochemical biosensor, the stepwise construction process was characterized by Nyquist plots of electrochemical impedance spectroscopy (EIS) and cyclic voltammograms (CVs), and the results are shown in Figs. 2A and S2. The bare GE revealed a negligible semicircle of EIS and a pair of reversible redox peaks of $[Fe(CN)_6]^{-3/-4}$, reflecting its good charge-transfer (curve a). When the GE was modified with Ab_1 and BSA, the redox peak current decreased and the interfacial charge-transfer resistance (R_{et}) increased, suggesting that the electron transfer was suppressed by Ab_1 and BSA (curve b). After HCVcAg was incubated with the prepared electrodes, the R_{et} continually increased and the CV value further decreased (curve c), indicating that HCVcAg was bound to Ab_1. The R_{et} and redox peak current continued to change after recognizing with DNA-Ab_2 (curve d). Adding TdT and dTTPs to the electrodes, a reduced CV response and an increased R_{et} were observed, suggesting that TdT amplification could produce long DNA strands (curve e). The change was attributed to the repulsive reaction between negative charged $[Fe(CN)_6]^{-3/-4}$ and DNA, which impeded electron transfer. Furthermore, DPV signals of the electrochemical biosensor responding to HCVcAg and blank control were recorded, and the results were depicted in Fig. 2B. Compared to the blank control experiment, an obviously improved current intensity was observed in the presence of HCVcAg. These results demonstrated that the developed electrochemical biosensor was feasible for the detection of HCVcAg.

Optimization of experimental conditions

To gain the excellent detection performance of the biosensor, several important reaction parameters were optimized systematically. (1) First, the concentration of Ab_1 was studied, because it determined the efficiency of the binding of HCVcAg to the electrode surface. As shown in Fig. 3A, the DPV signal gradually improved with the increase of Ab_1 concentration from 5 to 50 μg/mL, and remained stable at the higher Ab_1 concentration. According to these results, 50 μg/mL Ab_1 made the biosensor achieve the highest DPV signal, which thus was chosen as the optimal concentration. (2) Then, various concentrations of TdT

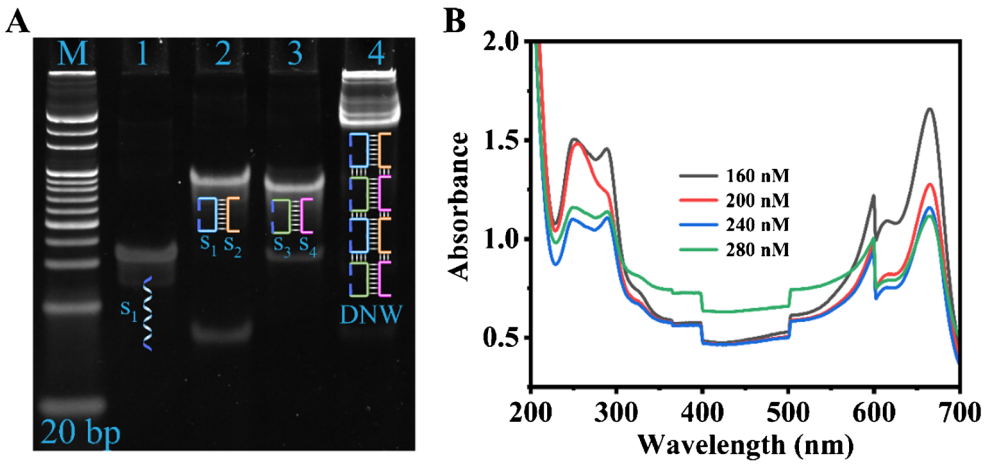

Fig. 1 **A** Characterization of DNW by using PAGE: (M) 20 bp marker, (1) S1, (2) S1 + S2, (3) S3 + S4, (4) S1 + S2 + S3 + S4. The concentrations of all DNA substrates were 1.0 μM. B Loading MB into DNW: the UV–vis adsorption spectrum of MB (1.0 μM) solution in the presence of different concentrations of DNW ranging from 160 to 280 nM. The incubation time was 2.0 h

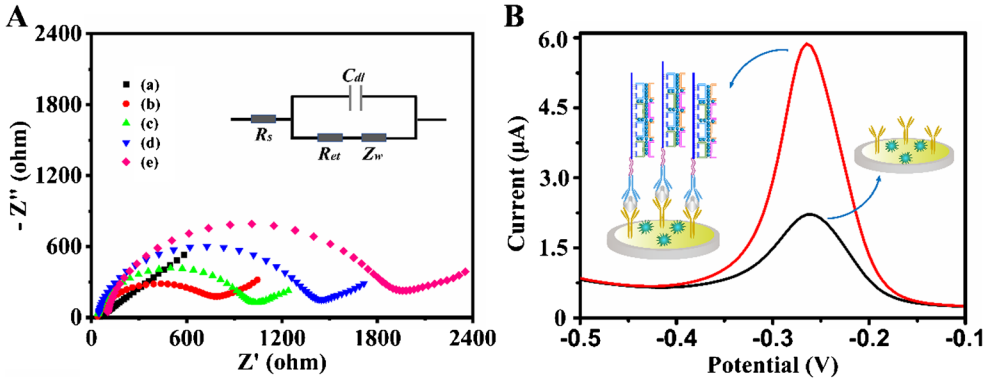

Fig. 2 Valuation of the feasibility of the electrochemical biosensor. **A** Nyquist plots of the biosensor construction process in 5×10^{-3} M $[Fe(CN)_6]^{-3/-4}$ containing 0.4 M KCl at (a) GE, (b) BSA/Ab_1/GE, (c) HCVcAg/BSA/Ab_1/GE, (d) DNA-Ab_2/HCVcAg/ BSA/Ab_1/GE, and (e) TdT/DNA-Ab_2/HCVcAg/BSA/Ab_1/GE. Inset is the equivalent circuit for Nyquist plots, in which *Rs* is the solution resistance, C_{dl} is the double layer capacitance, R_{et} is the charge-transfer resistance, and Z_w is the Warburg impedance. **B** DPV curves responding to target and blank control. The concentrations of DNA-Ab_2, dTTPs, TdT, and target were 20 nM, 0.5 mM, 5 U/μL, and 0.35 ng/mL, respectively. Analytical DPV signals were measured at the peak, that is around −0.25 V (Ag/AgCl)

were evaluated, because it directly affected the extended efficiency of DNA chain. As shown in Fig. 3B, an upward trend in the DPV signal was observed from 2.0 to 5.0 U/μL TdT; after which, the signal intensity showed ignorable change. Thus, 5.0 U/μL TdT was demonstrated to be optimized for the developed biosensor. (3) Subsequently, the reaction time of TdT was studied, due to the fact that it determined the length of the extended DNA strand. As depicted in Fig. 3C, the DPV signal increased dramatically as the incubation time increased from 15 to 60 min, while the signal decreased obviously at the longer reaction time. This is probably because overlong DNA strands tended to aggregate, leading to the frustrated binding of signal tags to the extended strand. Therefore, 60 min was selected as the optimized reaction time of TdT. (4) Finally, the concentration of MB@DNW was optimized. As illustrated in Fig. 3D, the DPV signal had an increasing trend from 0.1 to 0.6 μM of MB@DNW, and then the signal remained stable. Thus, we adopted 0.6 μM of MB@DNW for the following experiments.

Analytical performance of the electrochemical biosensor

To evaluate the analytical performance of the electrochemical biosensor for HCVcAg, various concentrations of

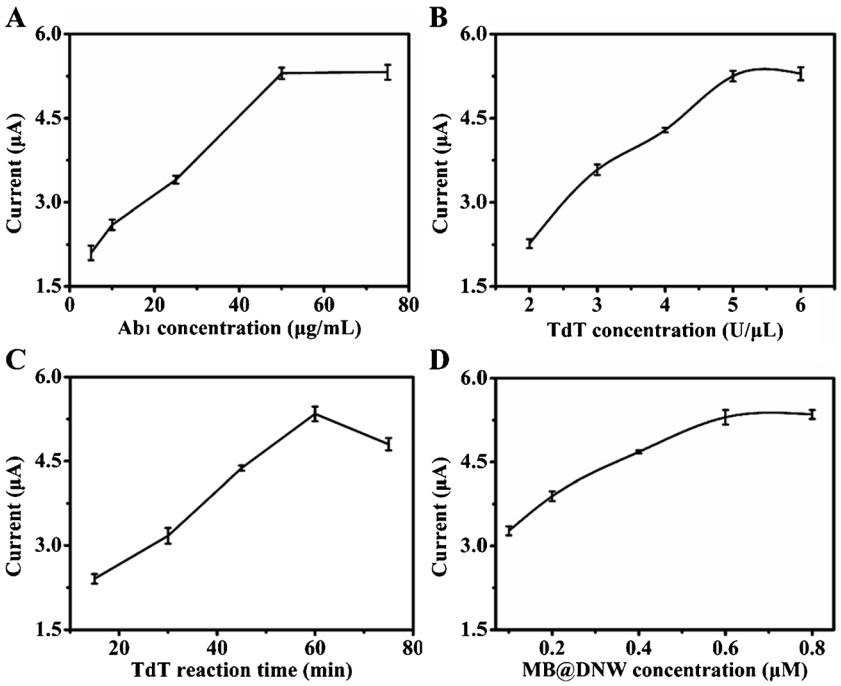

Fig. 3 Optimization of the reaction conditions: the effect of (**A**) Ab_1 concentration, (**B**) TdT concentration, (**C**) reaction time of TdT, and (**D**) MB@DNW concentration on the DPV signal. The concentration of HCVcAg was 312.5 pg/mL. Error bars are standard deviations obtained from three independent experiments conducted on three different electrodes

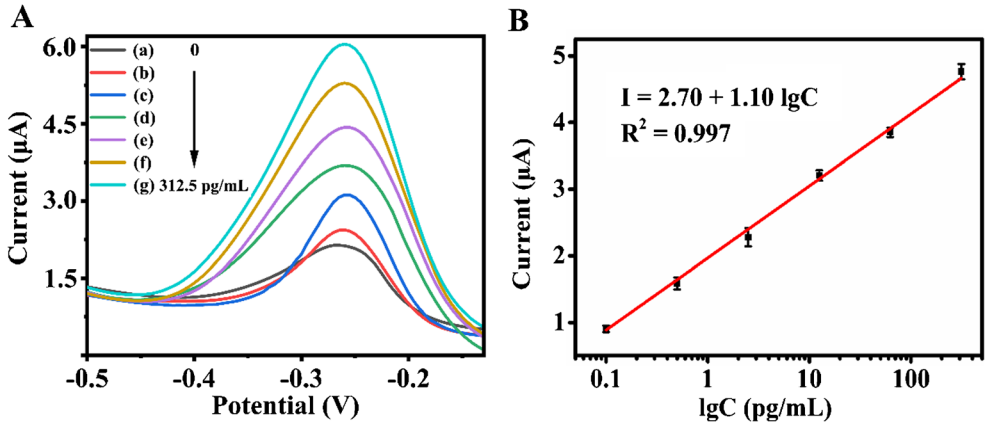

Fig. 4 Evaluation of the sensitivity of the biosensor. **A** DPV signals responding to different target concentrations: (a) 0, (b) 0.1 pg/mL, (c) 0.5 pg/mL, (d) 2.5 pg/mL, (e) 12.5 pg/mL, (f) 62.5 pg/mL, and (g) 312.5 pg/mL HCVcAg. **B** Linear relationship between the DPV signal and the logarithm of HCVcAg concentration from 0.1 to 312.5 pg/mL. Analytical DPV signals were measured at the peak, that is around −0.25 V (Ag/AgCl). Error bars are standard deviation obtained from three independent experiments conducted on three different electrodes

HCVcAg were tested under the optimized reaction conditions. As shown in Fig. 4A, the DPV signal gradually improved as the concentration of HCVcAg increased from 0 to 312.5 pg/mL, indicating that the produced DPV signal depended on HCVcAg concentration. As shown in Fig. 4B, the biosensor exhibited a good linear relationship between the DPV signal and the logarithm of HCVcAg concentration ranging from 0.1 to 312.5 pg/mL. The corresponding linear equation was $I = 2.70 + 1.10 \lg C$ ($R^2 = 0.997$), where I refers to the DPV current intensity and c indicates HCVcAg concentration. The standard deviation of the sensitivity and intercept of the linear equation were 0.03 and 0.04, respectively. The limit of detection (LOD) was calculated to be 32.0 fg/mL on the basis of the expression $S/N = 3$. Compared with other reported biosensors for HCVcAg analysis, the developed biosensor showed comparable or even superior performance in terms of LOD and linear detection range (Table S2). Moreover, the sensitivity of the biosensor was much better than that of the commercial ELISA kit (5 pg/mL). The excellent performance of the biosensor primarily benefited from the integration of the TdT amplification system and MB@DNW.

Specificity, stability, and repeatability of the biosensor

To evaluate the specificity of the electrochemical biosensor, some interfering proteins were tested, such as HCV structural protein (c22), HCV non-structural protein (NS4), HBV surface antigen (HBsAg), and immunoglobulin G (IgG). As shown in Fig. 5A, the DPV intensity of these interfering proteins was almost the same as that of the blank control, while the DPV signal enhanced distinctly in the presence of HCVcAg. These results demonstrated that the biosensor possessed good specificity for HCVcAg detection and could avoid the interference of other proteins. Furthermore, to evaluate the stability of the biosensor, 18 prepared electrodes and MB@DNW were placed at 4 °C, and TdT was stored at −20 °C. At intervals of 3 days, three different electrodes were taken out and then measured in response to 2.5 pg/mL HCVcAg. As illustrated in Fig. 5B, although the components of the developed biosensor were stored for 15 days, the electrochemical signal had small undulation. Therefore, the good stability of the electrochemical biosensor was demonstrated. In addition, to investigate the repeatability of the biosensor,

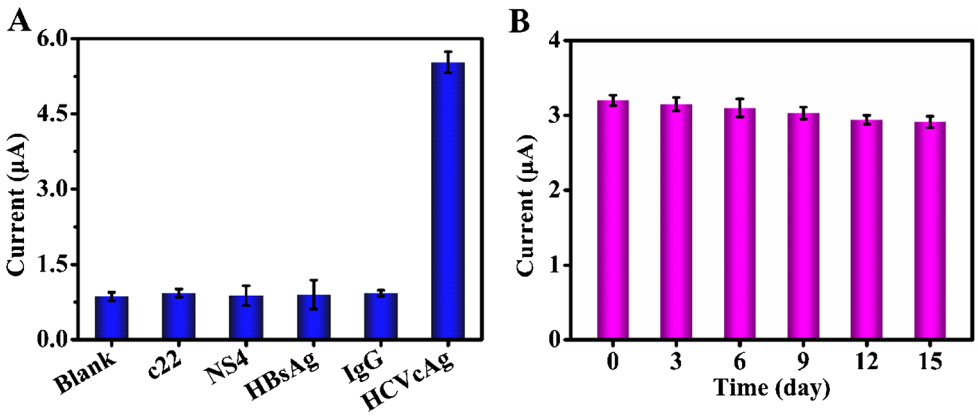

Fig. 5 **A** Evaluation of the specificity of the biosensor: DPV signals of blank control, four interferences (5.0 ng/mL), and HCVcAg (312.5 pg/mL). **B** Evaluation of the stability of the biosensor: DPV signals responding to 12.5 pg/mL HCVcAg from 1 to 15 days. Error bars are standard deviations obtained from three independent experiments conducted on three different electrodes

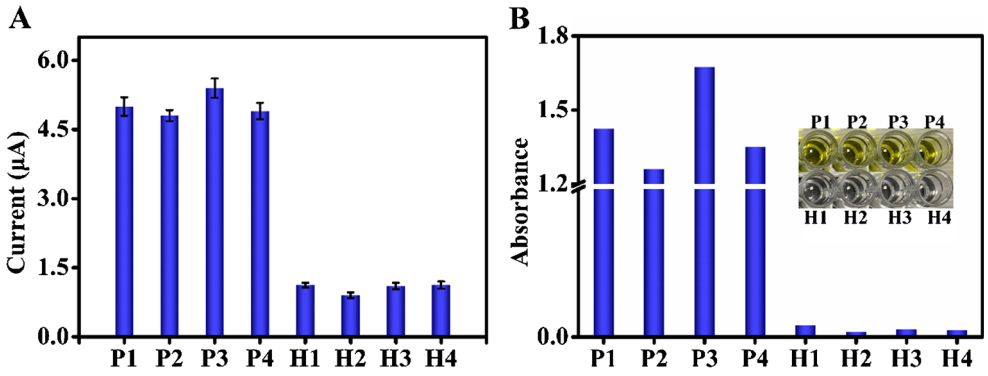

Fig. 6 Evaluation of the practicability of the biosensor. Detection of HCVcAg from HCV patients (P1–P4) and healthy volunteers (H1-H4) by (**A**) the developed biosensor and (**B**) the ELISA kit

five different electrodes were tested for 12.5 pg/mL HCVcAg, and the relative standard deviation (RSD) of the signal values was analyzed. The RSD was calculated to be 4.1%, indicating that the developed biosensor had good repeatability.

Clinical application of the electrochemical biosensor

To evaluate the practicability of the biosensor, the standard addition experiment was first performed by adding various concentrations of HCVcAg to diluted healthy serum samples. As shown in Table S3, the recoveries ranged from 98.0 to 104% with the RSD of 2.5–4.4%. These results demonstrated that the constructed electrochemical biosensor possessed good accuracy for the detection of HCVcAg in serum samples. The good analytical performance of the biosensor powered us to further evaluate its feasibility in clinical samples. Eight clinical serum samples (4 HCV patients and 4 healthy volunteers) were collected from our hospital, and these samples were parallelly analyzed by the developed biosensor and ELISA kit. As shown in Fig. 6, the results of the electrochemical biosensor were consistent with that of ELISA, and the testing value of HCVcAg from HCV patients (P1–P4) obviously enhanced compared with healthy volunteers (H1–H4). These results demonstrated that our developed biosensor could be applied to analyze HCVcAg in clinical samples. Although this strategy holds good potential in practical application, some limitations remain: the preparation of electrodes was complex, and the modified electrodes cannot be used repeatedly.

Conclusion

We successfully constructed a new electrochemical biosensor based on TdT reaction as signal amplification and MB@DNW as a signal label for ultrasensitive HCVcAg analysis. Compared to other HCVcAg sensing strategies reported previously, the method we developed was easy to operate and has good reproducibility due to the lack of need for nanomaterials. The DNA nanowire was easily assembled by four short DNA chains, which could be label-free and have efficient load amounts of MB. Benefiting from TdT amplification–induced MB@DNW linkage, the biosensor achieved reliable and ultrasensitive detection of HCVcAg with the detection limit down to femtomole level. More importantly, through a recovery test and comparison with ELISA, the feasibility of the biosensor for HCVcAg detection in clinical samples was verified. Therefore, the developed electrochemical strategy offers a potential tool for accurate and sensitive detection of HCVcAg in the clinic.

Supplementary Information The online version contains supplementary material available at https://doi.org/10.1007/s00604-021-04939-2.

Funding This work was supported by the Natural Science Foundation of Chongqing (cstc2020jcyj-msxmX0764), the Combined Medical Funding of Chongqing Health Commission & Science and Technology Bureau (2020FYYX060), and the Xinglin Scholar Research Premotion Project of Chengdu University of TCM (YYZX2019067).

Compliance with ethical standards

Conflict of interest The authors declare that they have no competing of interests.

References

1. Dore GJ, Martinello M, Alavi M, Grebely J (2020) Global elimination of hepatitis C virus by 2030: why not? Nat Med 26:157–160
2. Ge D, Fellay J, Thompson AJ (2009) Genetic variation in IL28B predicts hepatitis C treatment-induced viral clearance. Nature 461: 399–401
3. Hanafiah KM, Groeger J, Flaxman AD, Wiersma ST (2013) Global epidemiology of hepatitis C virus infection: new estimates of age-specific antibody to HCV seroprevalence. Hepatology 57:1333–1342
4. Fabrizi F, Lunghi G, Aucella F, Mangano S, Barbisoni F, Bisegna S, Vigilante D, Limido A, Martin P (2005) Novel assay using total hepatitis C virus (HCV) core antigen quantification for diagnosis of HCV infection in dialysis patients. J Clin Microbiol 43:414–420
5. Seme K, Poljak M, Babic DZ, Mocilnik T, Vince A (2005) The role of core antigen detection in management of hepatitis C: a critical review. J Clin Virol 32:92–101
6. Bouvier-Alias M, Patel K, Dahari H, Beaucourt S, Larderie P, Blatt L, Hezode C, Picchio G, Dhumeaux D, Neumann AU, McHutchison JG, Pawlotsky JM (2002) Clinical utility of total

HCV core antigen quantification: a new indirect marker of HCV replication. Hepatology 36:211–218
7. Kaiser T, Damerow HC, Tenckhoff S, Finger A, Böttcher I, Hafer C, Schwarz A, Lüth JB, Schmidt Gürtler H, Colucci G, Manns MP, Wedemeyer H, Tillmann HL (2008) Kinetics of hepatitis C viral RNA and HCV-antigen during dialysis sessions: evidence for differential viral load reduction on dialysis. J Med Virol 80:1195–1201
8. Schüttler CG, Thomas C, Discher T, Friese G, Lohmeyer J, Schuster R, Schaefer S, Gerlich WH (2004) Variable ratio of hepatitis C virus RNA to viral core antigen in patient sera. J Clin Microbiol 42:1977–1981
9. Orito E, Mizokami M, Tanaka T, Lau JY, Suzuki K, Yamauchi M, Ohta Y, Hasegawa A, Tanaka S, Kohara M (1996) Quantification of serum hepatitis C virus core protein level in patients chronically infected with different hepatitis C virus genotypes. Gut 39:876–880
10. Valipour A, Roushani M (2017) TiO_2 nanoparticles doped with Celestine Blue as a label in a sandwich immunoassay for the hepatitis C virus core antigen using a screen printed electrode. Microchim Acta 184:2015–2022
11. Valipour A, Roushani M (2017) A glassy carbon immunoelectrode modified with vanadium oxide nanobelts for ultrasensitive voltammetric determination of the core antigen of hepatitis C virus. Microchim Acta 184:4477–4483
12. Valipour A, Roushani M (2017) Using silver nanoparticle and thiol graphene quantum dots nanocomposite as a substratum to load antibody for detection of hepatitis C virus core antigen: electrochemical oxidation of riboflavin was used as redox probe. Biosens Bioelectron 89:946–951
13. Ghanbari K, Roushani M (2018) A nanohybrid probe based on double recognition of an aptamer MIP grafted onto a MWCNTs-Chit nanocomposite for sensing hepatitis C virus core antigen. Sens Actuators B-Chem 258:1066–1071
14. Li X, Yin C, Wu Y, Zhang Z, Jiang D, Xiao D, Fang X, Zhou C (2020) Plasmonic nanoplatform for point-of-care testing trace HCV core protein. Biosens Bioelectron 147:111488
15. Li X, Iocozzia J, Chen Y, Zhao S, Cui X, Wang W, Yu H, Lin S, Lin Z (2018) From precision synthesis of block copolymers to properties and applications of nanoparticles. Angew Chem Int Ed Eng 57:2046–2070
16. Xiao M, Lai W, Man T, Chang B, Li L, Chandrasekaran AR, Pei H (2019) Rationally engineered nucleic acid architectures for biosensing applications. Chem Rev 119:11631–11717
17. Wang W, Yu S, Huang S, Bi S, Han H, Zhang JR, Lu Y, Zhu JJ (2019) Bioapplications of DNA nanotechnology at the solid-liquid interface. Chem Soc Rev 48:4892–4920
18. Li F, Zhou Y, Yin H, Ai S (2020) Recent advances on signal amplification strategies in photoelectrochemical sensing of microRNAs. Biosens Bioelectron 166:112476
19. Zeng Z, Zhou R, Sun R, Zhang X, Cheng Z, Chen C, Zhu Q (2020) Nonlinear hybridization chain reaction-based functional DNA nanostructure assembly for biosensing, bioimaging applications. Biosens Bioelectron 173:112814
20. Wang H, Wang H, Willner I, Wang F (2020) High-performance biosensing based on autonomous enzyme-free DNA circuits. Top Curr Chem 378:20
21. Ge Z, Gu H, Li Q, Fan C (2018) Concept and development of framework nucleic acids. J Am Chem Soc 140:17808–17819
22. Huang X, Niu W, Wu J, Wang Y, Li C, Qiu J, Xue J (2019) A triple-amplification differential pulse voltammetry for sensitive detection of DNA based on exonuclease III, strand displacement reaction and terminal deoxynucleotidyl transferase. Biosens Bioelectron 143:111609
23. Wang L, Pan Y, Liu Y, Sun Z, Huang Y, Li J, Yang J, Xiang Y, Li G (2020) Fabrication of an aptamer-coated liposome complex for the detection and profiling of exosomes based on terminal deoxynucleotidyl transferase-mediated signal amplification. ACS Appl Mater Interfaces 12:322–329
24. Chen X, Cao G, Wang X, Ji Z, Xu F, Huo D, Luo X, Hou C (2020) Terminal deoxynucleotidyl transferase induced activators to unlock the trans-cleavage of CRISPR/Cpf1 (TdT-IU-CRISPR/Cpf1): an ultrasensitive biosensor for Dam MTase activity detection. Biosens Bioelectron 163:112271
25. Zheng J, Shi H, Wang M, Duan C, Huang Y, Li C, Xiang Y, Li G (2020) Homogenous electrochemical method for ultrasensitive detection of tumor cells designed by introduction of poly(A) tails onto cell membranes. Anal Chem 92:2194–2200
26. Lei S, Liu Z, Xu L, Zou L, Li G, Ye B (2020) A "signal-on" electrochemical biosensor based on DNAzyme-driven bipedal DNA walkers and TdT-mediated cascade signal amplification strategy. Anal Chim Acta 1100:40–46
27. Li X, Du Z, Lin S, Tian J, Tian H, Xu W (2020) ExoIII and TdT dependent isothermal amplification (ETDA) colorimetric biosensor for ultra-sensitive detection of Hg^{2+}. Food Chem 316:126303
28. Liu Q, Ge Z, Mao X, Zhou G, Zuo X, Shen J, Shi J, Li J, Wang L, Chen X, Fan C (2018) Valency-controlled framework nucleic acid signal amplifiers. Angew Chem Int Ed Eng 57:7131–7135
29. Liu P, Qian X, Li X, Fan L, Li X, Cui D, Yan Y (2020) Enzyme-free electrochemical biosensor based on localized DNA Cascade displacement reaction and versatile DNA nanosheets for ultrasensitive detection of exosomal MicroRNA. ACS Appl Mater Interfaces 12:45648–45656
30. Zhao Y, Hu S, Wang H, Yu K, Guan Y, Liu X, Li N, Liu F (2017) DNA dendrimer-streptavidin nanocomplex: an efficient signal amplifier for construction of biosensing platforms. Anal Chem 89: 6907–6914
31. Rahbani JF, Hariri AA, Cosa G, Sleiman HF (2015) Dynamic DNA nanotubes: reversible switching between single and double-stranded forms, and effect of base deletions. ACS Nano 9:11898–11908
32. Hariri AA, Hamblin GD, Gidi Y, Sleiman HF, Cosa G (2015) Stepwise growth of surface-grafted DNA nanotubes visualized at the single-molecule level. Nat Chem 7:295–300
33. Jiang Q, Song C, Nangreave J, Liu X, Lin L, Qiu D, Wang ZG, Zou G, Liang X, Yan H, Ding B (2012) DNA origami as a carrier for circumvention of drug resistance. J Am Chem Soc 134:13396–13403
34. Xue C, Zhang S, Yu X, Hu S, Lu Y, Wu ZS (2020) Periodically ordered, nuclease-resistant DNA nanowires decorated with cell-specific aptamers as selective theranostic agents. Angew Chem Int Ed Eng 59:17540–17547
35. Zong C, Wu J, Liu M, Yang L, Yan F, Ju H (2014) Chemiluminescence imaging for a protein assay via proximity-dependent DNAzyme formation. Anal Chem 86:9939–9944
36. Wang B, Shi S, Yang X, Wang Y, Qi H, Gao Q, Zhang C (2020) Separation-free electrogenerated chemiluminescence immunoassay incorporating target assistant proximity hybridization and dynamically competitive hybridization of a DNA signal probe. Anal Chem 92:884–891
37. Zhou Z, Xiang Y, Tong A, Lu Y (2014) Simple and efficient method to purify DNA-protein conjugates and its sensing applications. Anal Chem 86:3869–3875
38. Wang X, Gao H, Qi H, Gao Q, Zhang C (2018) Proximity hybridization-regulated immunoassay for cell surface protein and protein-overexpressing cancer cells via electrochemiluminescence. Anal Chem 90:3013–3018